RSC Advances

PAPER

Cite this: *RSC Adv.*, 2015, **5**, 63345

Modification of *Rapana thomasiana* hemocyanin with choline amino acid salts significantly enhances its antiproliferative activity against MCF-7 human breast cancer cells†

Maya Guncheva,*[a] Krasimira Paunova,[a] Paula Ossowicz,[bc] Zbigniew Rozwadowski,[c] Ewa Janus,[b] Krassimira Idakieva,[a] Svetla Todinova,[d] Yuliana Raynova,[a] Veselina Uzunova,[d] Sonia Apostolova,[d] Rumiana Tzoneva[d] and Denitsa Yancheva[a]

Received 24th June 2015
Accepted 20th July 2015

DOI: 10.1039/c5ra12214g

www.rsc.org/advances

This is the first study on the interactions of ionic liquids with large metalloproteins, in particular hemocyanins (Hcs). At first, complexes of a Hc from *Rapana thomasiana* (RtH) with a series of biocompatible choline amino acid salts [Chol][AA] were obtained. Applying UV-vis spectroscopy, Fourier-transformed infrared spectroscopy and differential scanning calorimetry the effect of these organic salts on the structure and thermal stability of RtH was assessed. Then, the cytotoxic effect of RtH–[Chol][AA] on breast cancer cells (MCF-7) and 3T3 fibroblast cells (non cancerous) was evaluated. We found that all [Chol][AA] induced clear time- and concentration-dependent alterations in the RtH conformation. The conformation and the thermal stability of IL-modified RtH depend strongly on the type of the anion of the tested compounds. All [Chol][AA]-modified RtHs exhibited lower thermal stability than the native RtH. At the same time, we established a good correlation between the structure of RtH and its antitumor activity. Namely, RtH–[Chol][AA] complexes exhibited enhanced antiproliferative activity toward the MCF-7 cell line. The observed antiproliferative effect was cell specific and the compounds have no effect or in some cases have stimulatory effect on fibroblasts.

1. Introduction

Hemocyanins (Hcs) are respiratory type-3 copper proteins found in the hemolymph of molluscs and arthropods. Molecules of molluscan Hcs are structured as decamers (cephalopods) or didecamers (gastropods) of subunits, all comprising of eight functional units (FUs). Each FU contains a binuclear copper active site, complexed with six histidine residues, and capable to bind dioxygen reversibly.[1] Hcs are known for their remarkable immunostimulating and immunomodulating properties and some of them are successfully used in oncotherapy and have potential as vaccine adjuvants.[2–4] The functionality of these respiratory proteins can be altered by modification of their structure and conformation. For example, it has been found that the modification of the Hc form limpet *Fissurella latimarginata* with sodium periodate enhanced its immunogenicity,[3] and Hc from scorpion *Pandinus imperator* acquired a phenoloxidase activity after treatment with sodium dodecyl sulfate.[5] In addition, it has been reported that treatment of a Hc from *Rapana thomasiana* (RtH) with detergents, resulted in a limited proteolysis or lyophilization induced change in the protein conformation and enhanced enzyme activity.[6]

As can be seen, depending on the environment and the conditions, Hcs due to their complex structure can be involved in various chemical and biochemical reactions *e.g.* oxygen transportation, induction of immune response, development of biosensors, wound healing processes, *etc.* Not only the primary structure and carbohydrate composition but also the correct folding of the whole protein is indispensible factor responsible for its activity. It is noteworthy to be mentioned that, except the effect of SDS, the effect of other organic salts on the secondary structure and the biological activity of Hcs, particularly cell proliferation, have not been estimated yet.

Potentially good effectors for hemocyanin modification could be ionic liquids (ILs). They are molten salts comprising of an organic cation and an organic or an inorganic anion and characterize with melting points below 100 °C, low vapour

[a]*Institute of Organic Chemistry with Centre of Phytochemistry, Bulgarian Academy of Sciences, Acad. G. Bonchev Str. bl. 9, 1113 Sofia, Bulgaria. E-mail: maiag@orgchm.bas.bg; Fax: +359 28700225; Tel: +359 29606160*

[b]*Institute of Organic Chemical Technology, West Pomeranian University of Technology Szczecin, Pulaski Str. 10, 70-322 Szczecin, Poland*

[c]*Department of Inorganic and Analytical Chemistry, West Pomeranian University of Technology Szczecin, Piastow 42, 71-065 Szczecin, Poland*

[d]*Institute of Biophysics and Biomedical Engineering, Bulgarian Academy of Sciences, Acad. G. Bonchev Str., bl. 21, 1113 Sofia, Bulgaria*

† Electronic supplementary information (ESI) available. See DOI: 10.1039/c5ra12214g

pressures, excellent chemical and thermal stabilities. Due to their unique tuneable physicochemical properties, ILs find various applications in (bio)catalysis, drug delivery, separation technology, electrochemistry, CO_2 storage, solar cells, *etc.*[7–9] Among them, in recent years, the biotechnological application of ILs has attracted an increasing attention. There are numerous data on enhanced selectivity, activity and/or thermal stability of hydrolases and oxidoreductases in imidazolium-based and pyridinium-based ILs.[10,11] In addition, protein stability in protic ILs has been extensively studied and some promising results have been reported. For example, Byrne and Angell have found that ethyl ammonium nitrate is able to recover egg while lysozyme conformation and activity after severe denaturation leading to fibril formation.[12] Up to 69% increase in the lysozyme refolding yield has been observed in presence of *N*-alkyl-*N*-methylpyrrolidinium chlorides which is due to inhibition of the aggregation of the unfolded protein molecules *i.e.* enhancing kinetic stability of the lysozyme.[13] Böhm *et al.* have reported an oxidative folding of cardioactive peptide and μ-conotoxins isolated from *Conus villepinii* in aqueous solutions of 1-ethyl-3-methylimidazolium tosylate and 1-ethyl-3-methylimidazolium acetate.[14] Another example of beneficial effect of some ILs on proteins is choline dihydrogen phosphate, which has been shown to preserve the native conformation and to provide long-term stability to cytochrome C, as well as to enhance thermal stabilization, suppresses aggregation and enhances reversibility of ribonuclease A.[15,16] Kumar and Venkatesu have reported stabilization of the native conformation of insulin in several ammonium-based ILs as well as in 1-butyl-3-methylimidazolium chloride and 1-butyl-3-methylimidazolium bromide which they ascribed to protein–ILs interactions influencing the protein flexibility.[17,18] There are many other examples of beneficial effect of ILs with diverse structures that have stabilizing effect on the structure and the functionality of proteins and enzymes. At the same time, according to the literature many other ILs inhibit enzymes and/or have deleterious effect on the protein conformational, thermal and storage stability. The interactions between protein and ILs are complex and depend on the chemical structure and the physicochemical properties of the ILs, *e.g.* their polarity, hydrophobicity, H-bonding capacity, size of the cation and the anion, *etc.*[19,20] All this implies that ILs, especially those consisting of non-toxic and biocompatible cations and anions, may have potential to stabilize therapeutic proteins. In the future such ILs may find applications as excipients in drug formulations helping/aiming to improve their storage stability (shelf-life), to overcome some problems such as low solubility, aggregation, denaturation under the production conditions, *etc.*

Most of the experiments described in the literature, however, are focused on model small globular proteins. Yet, the mechanisms of protein stabilization, especially when it comes to large protein complexes, are not still clear and are disputable. In this paper, we aim to examine the effect of a series biocompatible ILs containing choline cation and amino acid anion [CholAA] on the conformational stability and the antiproliferative activity of a Hc from a marine snail *Rapana thomasiana* (RtH). At first, the target biocompatible compounds were synthesized, isolated and characterized. Then, we observed the complex formation between each ILs and RtH at various protein : IL ratios by UV-vis spectroscopy. Subsequently, using Fourier transform infrared spectroscopy, we followed the effect of [Chol][AA] on the secondary structure of RtH. The thermal stability of the IL-treated RtH was estimated calorimetrically. Finally, the effect of the pure RtH, CholAA-modified RtH, as well as those of the pure ILs on cell viability of MCF-7 breast cancer cells and 3T3 murine fibroblasts was assayed in MTT assay. This study provides an insight into the relationship between the structure of RtH and its anti-cancer activity, a result of both fundamental and practical interest.

2. Material and methods

2.1. Materials

Cholinium chloride [Chol][Cl] (≥97 wt%) was provided by Fluka. Amino acids – L-Met, Gly, L-Val, L-Leu, L-Thr, L-Ile, L-Trp, a purity of 99 wt% and higher were purchased from Carl Roth. DMSO-d6 and Dowex Monosphere 550 A UPW (OH form) resin were provided by Sigma-Aldrich. Absolute ethanol (99.8%) was purchased from Chempur.

Murine embryotic fibroblast (3T3) and human breast cancer (MCF-7) cell lines were purchased from American Type Culture Collection (ATCC).

Thiazolyl blue tetrazolium bromide (MTT) (98%) was purchased from Sigma. RPMI-1640, DMEM high glucose media, L-glutamine and sodium bicarbonate were purchased from PAN-Biotech GmbH, Aidenbach, Germany.

2.2. Synthesis and characterization of cholinium – based amino acid ionic liquids [Chol][AA]

The synthesis of seven [Chol][AA], namely: (2-hydroxyethyl)trimethylammonium L-methionate [Chol][Met], (2-hydroxyethyl) trimethylammonium glycinate[Chol][Gly], (2-hydroxyethyl)trimethylammonium L-valinate [Chol][Val], (2-hydroxyethyl)trimethylammonium L-leucinate [Chol][Leu], (2-hydroxyethyl) trimethylammonium L-threoninate [Chol][Thr], (2-hydroxyethyl)trimethylammonium L-isoleucinate [Chol][Ile] and (2-hydroxyethyl)trimethylammonium L-tryptophanate [Chol][Trp] consisted of two steps (Scheme 1). In the first step, chloride anion in cholinium chloride was exchanged to hydroxide anion on the ion exchange resin (Dowex Monosphere 550 A UPW (OH form) resin). In the second step, the so obtained choline hydroxide was reacted with the corresponding amino acid. The detailed synthetic procedure and characterization of the compounds are available as ESI.†

2.3. Isolation, purification of RtH and preparation of its complexes with the choline amino acid salts

The Hc used in this study was isolated from freshly obtained hemolymph of marine snails *Rapana thomasiana* by ultracentrifugation at 180 000 × *g* for 3 h at 4 °C, and subsequent purification using gel chromatography as previously described.[21] Protein concentration was determined spectrophotometrically

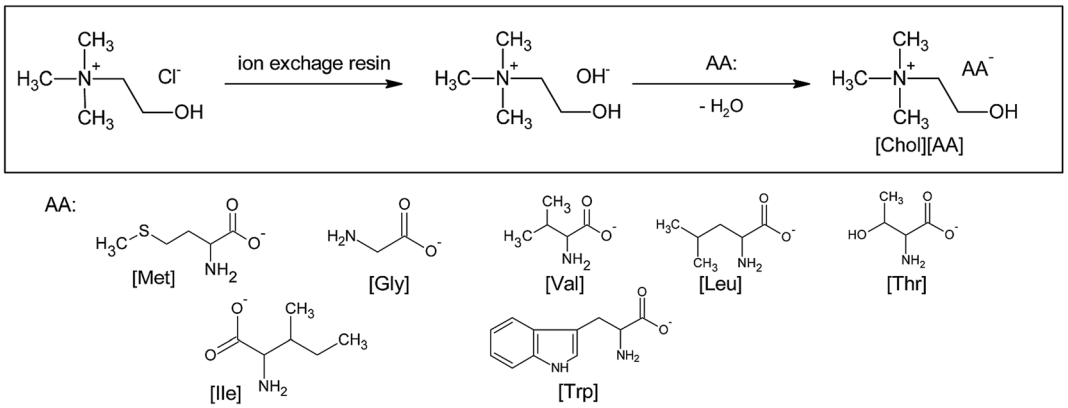

Scheme 1 Synthesis path and structures of cholinium-based amino acid ionic liquids [Chol][AA].

using the absorption coefficient $A_{278} = 1.36$ mg^{-1} mL cm^{-1} (20 °C).

To obtain protein–ILs samples, RtH (1.52 mg mL^{-1}) was incubated (0–48 h) with various amounts of the corresponding [Chol][AA] (0.01–0.4 M) at room temperature.

2.4. Polyacrylamide gel electrophoresis (PAGE)

RtH and its complexes with [Chol][AA] were subjected to SDS-PAGE analysis in 7.5% polyacrylamide gel as described by Laemmli.[22] Ovotransferrin (78.00 kDa), albumin (66.25 kDa), ovalbumin (42.70 kDa), carboanhydrase (30.00 kDa) (Merck), were used as molecular weight markers.

Native PAGE was conducted using the same conditions, but omitting the SDS from all buffers.

Silver staining was used to detect the proteins after electrophoretic separation on polyacrylamide gels.

2.5. UV-vis spectroscopy

Absorption spectra for RtH and its complexes with [Chol][AA] were recorded on Evolution™ 300 UV-vis Spectrophotometer (Thermo Electron Corporation) equipped with a Peltier temperature control accessory with the highest resolution (1 nm) using matched 1 cm path length quartz cuvettes. The protein concentration was kept constant (1.52 mg mL^{-1}; 0.17 μM) and the concentration of ILs was varied in the range 0.01–0.4 M. The reference cuvette was filled with sodium phosphate buffer (pH 7.2, 5 mM) and contained the same concentration of the corresponding IL. Repeat scanning was performed for each sample in order to follow the absorbance changes over time.

2.6. FTIR spectroscopy

FTIR spectra of the RtH (30.4 mg mL^{-1}) dissolved in sodium phosphate buffer (pH 7.2, 5 mM) or in 0.2 M aqueous solution of [Chol][AA] (in the same buffer) were recorded on Bruker Tensor 27 spectrometer, equipped with a detector of deuterated triglycine sulphate (DTGS). The FTIR spectra were collected by direct deposition of the samples on attenuated total reflectance (ATR) element (diamond crystal) in frequency region 4000–600 cm^{-1} (ATR) with 128 scanning and at resolution of 1 cm^{-1}. The spectra of the proteins were referenced to the respective spectra of 5 mM sodium phosphate buffer, pH 7.2, or 0.2 M solution of the corresponding IL in the same buffer in order to subtract their absorptions.

In order to describe quantitatively the changes in the RtH secondary structure induced by the [Chol][AA], the ATR-FTIR spectra were treated in accordance with the established methods given in the literature[23,24] ATR-FTIR spectra were Fourier deconvoluted by Opus software version 5.5 using bandwidth of 14 cm^{-1}, 2.9 resolution enhancement factor, and Lorentzian lineshape. Second derivative spectra were obtained using the Savitzky–Golay algorithm based on 25 smoothing points. Then, the relative contribution of each band component of the Amide I band was determined by curve fitting following the procedure of OPUS program. In the fitting, the number of components and the initial values of their position were set as determined from the second derivative spectra. The initial bandwidth of all components was set to 14 cm^{-1} and the components were approximated by mixed Lorentzian/Gaussian functions. The curve-fitting was performed according to the local least squares algorithm. The assignment of the Amide I band positions to secondary structure was done according to the literature data.[25]

2.7. Differential scanning calorimetry

DSC experiments were performed on DASM 4 (Privalov, BioPribor)-built-in highly sensitive calorimeter with cell volumes of 0.5 mL, a sensitivity >0.017 mJ K^{-1} and a noise level below 0.05 μW. An over-pressure of 2 atm was kept constant over the samples in the cells throughout the scans to avoid any degassing during heating. Each sample scan was preceded by a buffer run with buffer-filled cells. The obtained buffer scan was then used as base-line. The protein solutions in the calorimetric cell were reheated after the cooling from the first run to estimate the reversibility of the thermally induced transitions. All DSC measurements with RtH and RtH–ionic liquid complexes were carried out in 5 mM sodium phosphate buffer, pH 7.2 (20 °C) and heating rate of 1 K min^{-1}. Molecular mass of 9 MDa for RtH was used in the calculation of its molar concentration. As the thermal denaturation in all cases was found to be

calorimetrically irreversible, the second scan was used as baseline. The experimental curves were derived from the DSC thermograms by subtracting buffer–buffer scan (or second scan) and after normalizing by molar concentration of protein. The calorimetric data were evaluated using the ORIGIN 8. Each curve was deconvoluted mathematically, using theoretical Gaussian fitting. The temperature at the maximum of the excess heat capacity curve was taken as the main transition temperature (T_m).

2.8. Cell cultures conditions

In this study we used two cell lines: 3T3 murine fibroblasts were cultured in DMEM high glucose medium containing L-glutamine, penicillin–streptomycin–amphotericin B and 10% fetal bovine serum and breast cancer cell line MCF-7 were cultured in DMEM medium containing the same supplements and insulin. The cells were cultivated at humified atmosphere, 37 °C and 5% CO_2.

For the experimental procedures, cells were seeded in a sterile 96-well plate at 1×10^4 cells per well and incubated for 24 h at 37 °C and 5% CO_2 for obtaining adherent cell cultures and good cell spreading. Then, the cells were incubated for additional 24 h with non-treated RtH, pure [Chol][AA] or RtH–[Chol][AA] complexes, at concentrations ranging from 100–700 μg mL^{-1} and 0.67–4.7 mM for the protein complexes and pure ILs, respectively.

The RtH–[Chol][AA] complexes were obtained by incubation of 80 μL RtH (38 mg mL^{-1} stock) with 20 μL of 1 M aqueous solution of the corresponding [Chol][AA] at room temperature for 60 min.

2.9. Cytotoxicity assay by MTT

The viability of MCF-7 and 3T3 cells after their incubation with RtH and its complexes with the ILs was assessed in MTT colorimetric test.

The mitochondrial dehydrogenase activity is used to estimate the viability of cells. The enzyme converts a tetrazolium dye, 3-[4,5-dimethylthiazol-2-yl]-2,5-diphenyltetrazolium bromide, known as MTT, into formazan, a purple dye with an absorbance maximum near 570 nm. When cells die, they loss their ability to perform the reaction, thus colour formation serves as a marker for only viable cells, *i.e.* the quantity of the resultant formazan is proportional to the quantity of the viable cells.[26]

Routinely, 20 μL of tetrazolium dye was added directly to all 96-wells plates with the adherent cells. They were incubated for 3 h at 37 °C and 5% CO_2 and the absorbance at 570 nm was recorded with a 96-well plate reader Tecan Infinite F200 PRO (Tecan Austria GmbH, Salzburg). Blank experiments containing only reaction medium as well as control experiments with untreated MCF-7 and 3T3 cells were performed. The survival of the cells, treated with different concentrations of ChAAs and RtH–ChAAs complexes, was presented in percentages from the control (non-treated cells). Two independent experiments were performed for each cell line.

2.10. Statistical analysis

All statistical calculations were carried out with Graph Pad Prism software (Graph Pad Software Inc., San Diego, USA). Data were analysed by one-way ANOVA followed by Tukey–Kramer *post hoc* test. The values were considered to be significantly different if the p value was <0.05.

3. Results and discussion

3.1. Absorption spectra

RtH has two characteristic bands in its absorption spectra with maxima at 280 nm and 340 nm. The first one is mainly due to the aromatic amino residues of tryptophanes (Trp) and tyrosines (Tyr) from the protein. The second absorption band is typical for the oxygenated Hc and is attributed to the formation of copper–oxygen complex (Cu^{II}–O_2^{2-}–Cu^{II}).[27]

Similarly to other copper proteins and oxidoreductases, Hcs exist in two functional forms: oxygenated form (oxy-Hcs), which has two tetragonal Cu^{II} atoms in the active site, and deoxygenated form (deoxy-Hcs), which has bicuprous structure ($Cu^{I}Cu^{I}$) (Scheme S1†).[28] The relative abundance of the two forms depends on protein saturation with oxygen, and the fraction of the oxy-Hcs can be calculated from the absorbance ratio A_{340}/A_{280}, which varies among different Hcs from 0.21 to 0.28 according to the excitation coefficients of the individual bands. For the hemocyanin from *Rapana thomasiana*, A_{345}/A_{280} ratio as high as 0.25 is indicative of presence of only Hc in oxygenated form (100%).[27]

The wavelength and the strength of the band of the aromatic amino acid residues in the protein absorption spectra are sensitive to the environment. Therefore, we followed the changes in the absorption spectra of RtH in respect to the concentration of the tested [Chol][AA] (0.010–0.4 M) and the incubation time (0–48 h). The protein concentration in the cuvette was kept constant 1.52 mg mL^{-1} (*ca.* 0.17 μM) in all experiments. We observed that RtH treated with various concentrations of [Chol]-[AA] exhibited distinct changes compared to the native structure. The spectra of RtH in presence of various concentrations of [Chol]-[Gly], recorded immediately after mixing the protein and the IL, and the change of absorbance of RtH–[Chol][Gly] (0.01 M IL) over time are given as illustration in Fig. 1. For the RtH dissolved in sodium phosphate buffer (5 mM, pH 7.2) containing up to 0.2 M of the IL, we detected between 10 and 15% decline in the intensity of the absorption band ascribed to the aromatic residues of the protein, while in the solutions with higher IL concentration the loss of the strength of the band at 280 nm was about 20%. On one hand, the quenching of the absorption bands at 280 nm can be ascribed to conformational changes which lead to more compact structure in which Trp and Tyr residues are more buried inside the protein and are not exposed to the solvent. Similar effects have been observed by Attri *et al.* for α-chymotrypsin in protic ILs.[29] On the other hand, quenching of the Tyr and Trp absorbance may be due also to an aggregation of the partially unfolded protein molecules due to stronger hydrophobic interactions or H-bonding. For example, Kumar and Venkatesu have observed a denaturation and aggregation of insulin in presence of some imidazolium based ILs which led to a complete loss of Tyr absorption band in the UV-vis spectra of insulin.[18]

We found that small amounts of [Chol][Val] did not induce absorbance changes at 345 nm in the spectrum of RtH, while the same concentrations of all other tested ILs lowered A_{345}

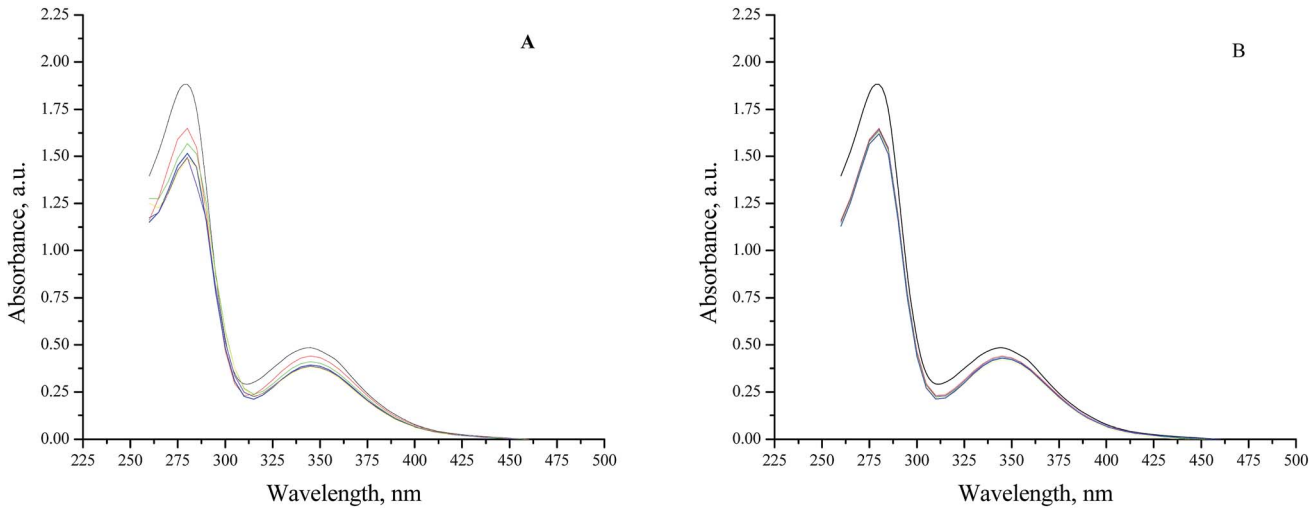

Fig. 1 (A) UV-vis absorbance of RtH (1.52 mg mL^{-1}), dissolved in sodium phosphate buffer (pH 7.2, 5 mM) containing various amounts of [Chol][Gly]: IL-free (black), 0.01 M (red), 0.05 M (blue), 0.1 M (violet), 0.2 M (green), 0.4 M (yellow) recorded immediately after protein–IL mixing. (B) Time evolved UV-vis absorption spectra of RtH, dissolved in sodium phosphate buffer (pH 7.2, 5 mM) containing 0.01 M [Chol][Gly]: 0 min (red), 20 min (blue), 40 min (magenta), 60 min (green), 24 h (yellow), and 48 h (grey). For comparison is given the spectrum of RtH in sodium phosphate buffer without IL (black).

intensity by 15–20% in respect to that of the native protein (Fig. S1†). It is noteworthy to be mentioned that the value of ratio A_{345}/A_{280} remains the same as for the non-treated with [Chol][AA] oxy-RtH and we assume that the oxygen binding properties of the protein are not affected. At higher concentration of ILs (>0.2 M), however, we observed a stronger effect of [Chol][AA] on the active site structure, *i.e.* we recorded a decrease in A_{345} intensity by 50% in presence of [Chol][Leu], by 40% in presence of 0.4 M [Chol][Gly] or [Chol][Met], and by 15% for the rests of ILs, which is probably due to lowering of the amount of copper(II)–peroxide complexes (Fig. S1†).

The conformational changes in RtH in presence of the tested choline amino acid salts occurred in first twenty minutes, except in the case of [Chol][Met], when longer incubation time (60 min) was needed to reach the new conformational equilibrium. Then, no changes in the absorption spectra of the RtH–[Chol][AA] complexes were observed even after a prolonged 48 h-incubation.

Therefore, based on the screening and initial experiments, we found suitable for the further experiments to keep constant the ratio of [Chol][AA] (10 mM) to RtH (1.52 mg mL^{-1}; 0.17 μM) and the incubation time of 60 minutes at 20 °C.

3.2. Effect of the choline amino acid salts on the secondary structure of RtH

We applied FTIR spectroscopy to monitor the induced by [Chol][AA] changes in the secondary structure of RtH. We followed the changes in Amide I region (1600–1700 cm^{-1}) of the infrared spectra, which is due mainly to C=O stretching vibrations (approx. 80%) and is very sensitive to changes in the geometry of amide bond and hydrogen bonding. For all samples, the main secondary structure elements were observed in the following frequency intervals: α-helical structures at 1650–1658 cm^{-1}, organized β-sheet structures and random at coils at 1620–1649 cm^{-1}, and distorted structures and antiparallel β-sheets at 1661–1696 cm^{-1}.

The percentages of each secondary structural element of the native RtH and RtH incubated with [Chol][AA] were calculated after deconvolution and fitting of each FTIR spectrum in the

Table 1 Quantitative estimation of the secondary structural elements of native hemocyanin from *Rapana thomasiana* and its complexes with choline-based amino acid salts calculated from their curve fitted FTIR spectra

Sample	α-Helix (%)	β-Sheet (%)	Random coils (%)	β-Turn (%)	H-bonded aggregates (%)	Amino acid side chains (%)
RtH	15.16	33.62	23.86	13.39	13.97	NA
RtH–[Chol][Gly]	14.67	28.80	15.38	8.85	22.58	9.72
RtH–[Chol][Val]	13.47	35.15	15.53	16.52	12.23	7.10
RtH–[Chol][Leu]	22.88	30.34	NA	26.62	9.74	10.42
RtH–[Chol][Ile]	14.36	28.47	NA	26.01	22.44	8.72
RtH–[Chol][Met]	NA	28.63	20.88	30.70	10.01	9.78
RtH–[Chol][Thr]	22.78	18.32	NA	48.13	10.77	NA
RtH–[Chol][Trp]	30.66	34.40	NA	15.28	19.89	NA

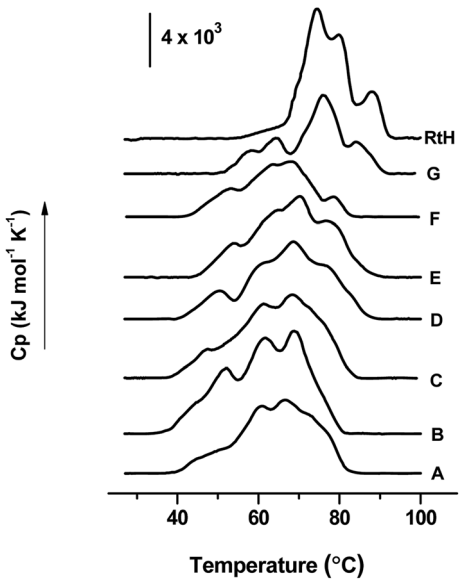

Fig. 2 DSC thermograms of native RtH in sodium phosphate buffer (pH 7.2, 5 mM) (on the top); RtH–ILs complexes: RtH–[Chol][Gly] (A); RtH–[Chol][Val] (B); RtH–[Chol][Leu] (C); RtH–[Chol][Ile] (D); RtH–[Chol][Met] (E); RtH–[Chol][Thr] (F); RtH–[Chol][Trp] (G). Experiments were performed at a heating rate of 1 °C min^{-1}.

Amide I region and the results are summarized in Table 1. The exact positions of the bands obtained after decomposition of the Amide I band into Gaussian components, as well as their original and curve fitted spectra are given for all samples as ESI (Fig. S2, Table S1).†

We found that all tested here ILs altered the secondary structure of RtH, which reflected in some spectral variations. For example, new bands, typically assigned to amino acid side chain (1602–1609 cm^{-1}) appeared in FTIR spectra of all RtH samples treated with ILs containing non-polar amino acid anions, *i.e.* glycyl, valyl, leucyl, isoleucyl and methionyl anions. This is probably due to partial unfolding of RtH upon which some of the hydrophobic side chains become more exposed to the solvent and are additionally stabilized by interactions with these organic salts. In addition, [Chol][Leu] induces noticeable conformational changes in RtH increasing the content of α-helical and β-structural elements on account of random coils and probably in this system the protein molecules are more tightly packed.

The most dramatic changes of the protein secondary structural elements, however, were observed in the system containing [Chol][Met]. The complete absence of α-helix peak in the frequency region 1650–1658 cm^{-1} (Table S1, Fig. S2†) and the presence of two strong peaks at 1661 and 1677 cm^{-1} which are assigned to β-turns and β-strands, resulted in the most non-native RtH structure within the tested series of compounds. In contrast, for the RtH incubated with [Chol][Trp], we observed a significant increase in α-helical structure (2-fold) at the expense of unordered structures while β-structural elements were preserved. The protein in this case underwent structural rearrangement leading to more ordered and compact state with hydrophobic/aromatic amino acid side chains buried in the core of protein. In comparison, FTIR spectra of RtH–[Chol][Thr] complexes showed a significant increase in the content of distorted secondary structures (β-turns, loose, β-strands) and moderate increase in α-helical content which we ascribed to serious β-rearrangement within the protein complex, thus we assume that this IL seriously disrupted RtH secondary structure.

All samples were subjected to native and SDS-PAGE to check whether the cholinium-based ILs caused a covalent bond cleavages and fragmentation of the huge Hc molecule (Fig. S3†). SDS-PAGE of the native RtH and RtH–[Chol][AA] complexes showed typical for this Hc electrophoretic patterns without indication for covalent bond cleavage (Fig. S3-A†). Native PAGE, however, demonstrated fragments with higher electrophoretic mobility, *i.e.* more negatively charged, in samples taken from RtH–[Chol][AA] compared with the native RtH (Fig. S3-B†).

3.3. DSC

Differential scanning calorimetry (DSC) was used to monitor changes in the thermodynamic state of proteins. We applied the method to follow the effect of the tested choline amino acid salts on the thermal unfolding of RtH. The DSC profiles of all samples are presented on Fig. 2. The complex unfolding is indication for the existence of more than one structural domain in the analyzed samples. Parameters characterizing the thermal unfolding of RtH under different reaction conditions, obtained by means of mathematical deconvolution of the curves, are given in Table 2. The deconvolution analysis, using theoretical

Table 2 Summary of DCS characteristics of four-component transition for the thermal unfolding process of RtH in presence of [Chol][AA], obtained from 2-state model

Sample	T_{m1} (°C)	ΔH_{1cal} (kJ mol^{-1})	T_{m2} (°C)	ΔH_{2cal} (kJ mol^{-1})	T_{m3} (°C)	ΔH_{3cal} (kJ mol^{-1})	T_{m4} (°C)	ΔH_{4cal} (kJ mol^{-1})	ΔH_{tot} (kJ mol^{-1})
RtH	72.9	32 688	74.5	64 386	80.6	26 183	87.8	20 222	141 571
RtH + [Chol][Gly]	50.5	27 511	59.6	31 055	67.5	55 586.4	75.6	24 852	136 354
RtH + [Chol][Val]	43.4	12 473	51.9	48 882	60.4	33 136.2	68.8	95 958	190 456
RtH + [Chol][Leu]	48.0	22 791	61.4	78 061	69.2	24 610.9	75.5	37 716	161 668
RtH + [Chol][Ile]	49.7	19 994	60.1	29 986	67.9	46 464.2	76.9	46 322	142 182
RtH + [Chol][Met]	52.5	18 001	64.3	67 103	70.3	15 087.5	77.6	45 737	144 917
RtH+ [Chol][Thr]	52.5	23 126	60.9	14 852	68.2	51 060.9	79.1	5087	93 801
RtH + [Chol][Trp]	57.1	9660	64.0	18 978	75.9	57 351	85.6	12 312	98 641

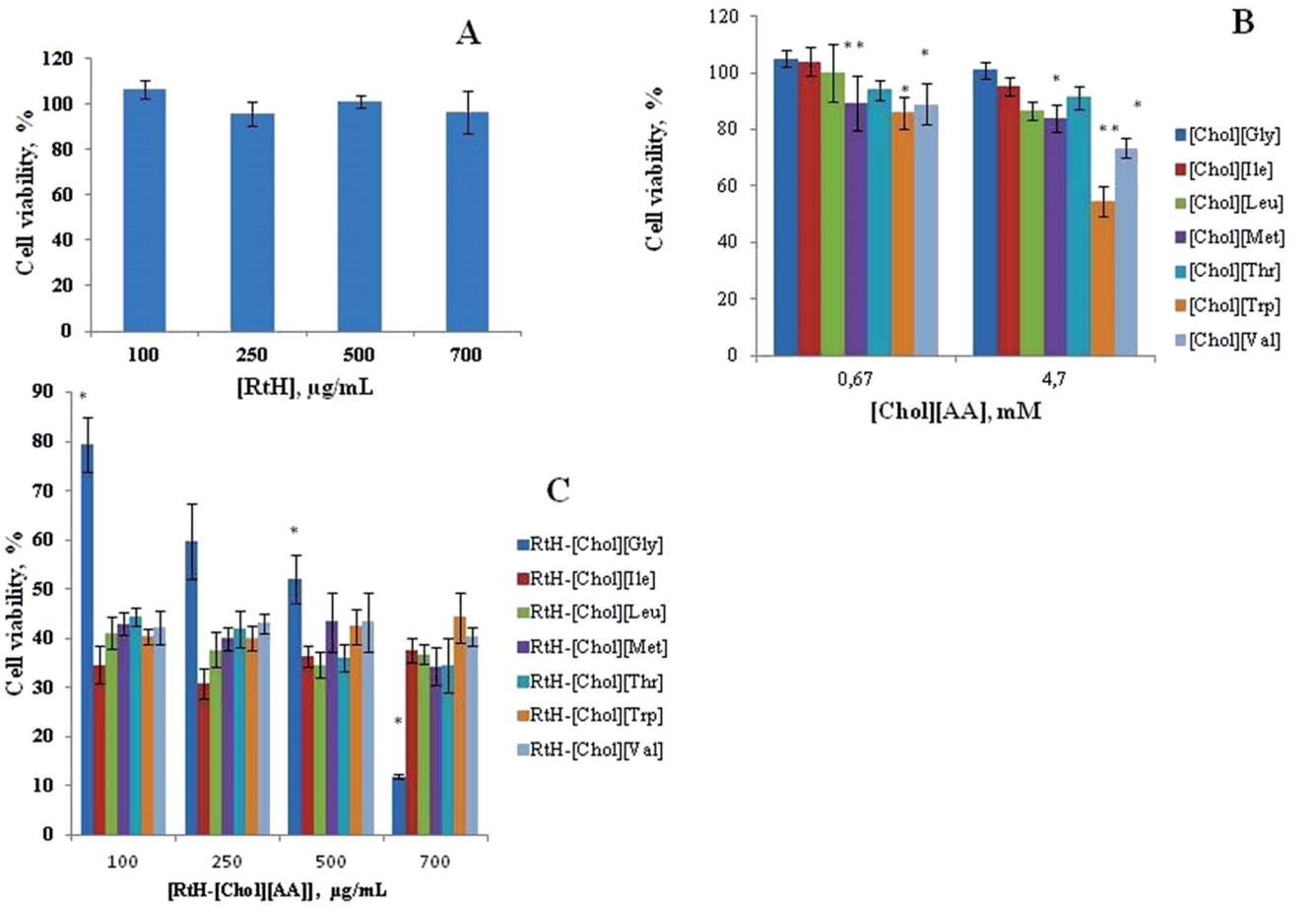

Fig. 3 Cell viability of MCF-7 after 24 h of incubation in presence of RtH (A), [Chol][AA] (B) and their complexes, RtH–[Chol][AA] (C). Data are means ± SD of eight replicates. The statistic was performed by ANOVA test. * – $p < 0.01$, ** – $p < 0.001$.

Gaussian fitting ($R = 0.998$), showed that the endotherms were well approximated as a sum of four independent transitions. The DSC thermogram of the RtH dissolved in 5 mM sodium phosphate buffer (pH 7.2) showed three endothermic maxima centered at 74.5, 80.6 and 87.8 °C and a lower temperature shoulder at 72.9 °C (Fig. S4-A,† Table 2). The result is in agreement with earlier reports where the multiple peak profile of RtH thermal denaturation was attributed to a simultaneous relatively independent unfolding of several structural domains or subunits.[30] As previously was suggested the sodium phosphate buffer possibly withdraws calcium and magnesium ions from the RtH and induces multi-stage dissociation of the protein.[30]

For all [Chol][AA]-treated RtH samples, we also observed that the denaturation was a complex process and in all experiments the maxima of the heat absorption were shifted toward lower temperatures (Fig. S4-B–H,† Table 2). The differences in their DSC profiles, we ascribe to the IL-induced changes in RtH secondary structure, *e.g.*, different degree of unfolding and/or different reorganization/rearrangement of secondary structural elements of the RtH subunits that were observed in FTIR spectra. The result is in agreement with the observed higher heterogeneity of the protein–IL complexes in comparison to non-treated RtH revealed by the native PAGE experiments (Fig. 3B).

We observed that the destabilizing effect of cholinium-based ILs depend strongly on anion structures and even small variations in their structure have significant impact on RtH conformational and thermal-stability. Overall, all of the tested organic salts can be ranked as follows: [Chol][Val] (the strongest denaturant, lower T_m) > [Chol][Leu] > [Chol][Ile] > [Chol][Gly] > [Chol]-[Met] ≈ [Chol][Thr] > [Chol][Trp] (Table 2).

At a first glance, the simple replacement of the hydroxyl group of L-threonine by methyl group in L-valine seems to have a dramatic effect on RtH conformation; subsequently, to its heat stability. In presence of cholinium valinate to the buffer system, however, we observed an exposure of hydrophobic structures, which are normally buried inside the protein to its surface. This conformational change is clearly seen from the changes in FTIR spectra of RtH–[Chol][Val] in the frequency region 1602–1609 cm^{-1} in comparison with the RtH FTIR spectra in buffer only (Fig. S2-A and C†). Thus, we assume that in the case of [Chol][Val] the hydrophobic interactions have a predominant contribution for the destabilization of this RtH–IL complex. On the other hand, [Chol][Thr] has also destabilizing effect on the RtH. However, due to its more polar nature, we assume that dipole–dipole interactions are predominant and are major driving forces for cholinium threonine–RtH binding interactions.

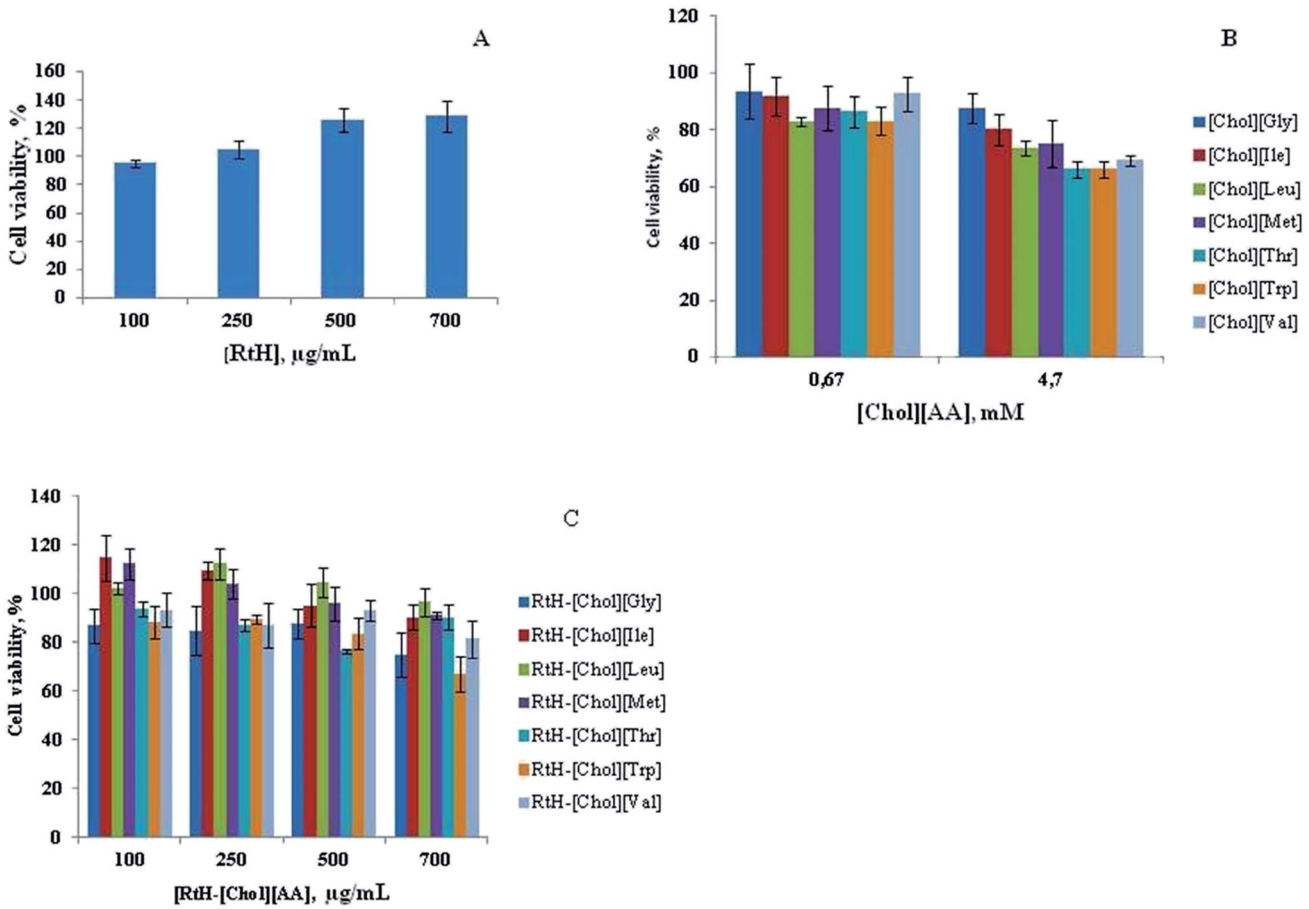

Fig. 4 Cell viability of 3T3 cells after 24 h of incubation in presence of RtH (A), [Chol][AA] (B) and their complexes, RtH–[Chol][AA] (C).

In addition, [Chol][Thr] may strip away the hydration shell surrounding the protein and maintaining its structure or to modify its properties; thus, altering RtH conformation.

It is known that even small variations in the structure of either cation or anion have a significant impact on physico-chemical and solvent properties of ILs.[31] The observed differences in DSC profiles are evidence that each tested cholinium-based amino acid salt modifies the RtH sample in a particular way due to its specific multipoint interaction with different region of the protein or subunits (Fig. 2).

3.4. Cell viability

The cytotoxic effects of the native and the pre-treated with ionic liquids RtHs on human breast cancer cells (MCF-7) and fibroblasts (3T3 cells, non-cancerous cells) were estimated at concentrations ranging from 100 μg mL^{-1} to 700 μg mL^{-1}. We performed also control experiments with samples containing only ionic liquids in concentrations of 0.67 mM and 4.7 mM, corresponding to the lowest and the highest amount of ILs introduced into the system with the RtH-complexes.

We found that the non-modified RtH had no effect on MCF-7 proliferation after 24 hour-treatment at the tested concentration range (Fig. 3A). In contrast, the native protein applied in the same concentration range exerted a stimulatory effect on the growth of 3T3 cells and the trend proved to be dose-dependent (Fig. 4A). In comparison, for the most studied and applied in prostate and bladder cancer conventional therapy hemocyanin from keyhole limpet, Riggs *et al.* have observed 38% of MCF-7 growth inhibition for 72 h after treatment of the cells with 500 μg mL^{-1} of KHL.[32]

To the best of our knowledge no studies are available in the literature on the effect of cholinium-based amino acid salts on MCF-7 and 3T3 cell proliferation. However, similar series of compounds, namely such containing cholinium cation and glycinate, D,L-alaninate, D,L-phenylalaninate, glutaminate, methionate, arginate or glutamate anion, have been previously tested by Gouveia *et al.* against human cervical carcinoma cells (HeLa). It is noteworthy to be mentioned that the authors reported on an increased cell growth in presence of all ILs even at concentrations as high as 30 mM.[33]

We found that most of the tested by us cholinium amino acid salts produced weak effects on MCF-7 cell growth after 24 hour-treatment. At low concentration of ILs (0.67 mM) the cell viability for all tested ILs was in the range of 80–100% *i.e.* rather high. Statistical reduction of cell viability was found in order: [Chol][Gly] ≈ [Chol][Ile] ≈ [Chol][Leu] > [Chol][Met] > [Chol][Trp] ≈ [Chol][Val]. At the same time, we observed a significant reduction in breast cancer cell viability (up to 50%) only with

[Chol][Trp] and moderate anti-proliferative activity (up to 25%) with [Chol][Met] and [Chol][Val] at concentration as high as 4.7 mM, which was the highest tested here (Fig. 3B). On contrary, tested toward fibroblasts (3T3 cells), [Chol][AA] resulted only in minor (10–20%) inhibition of cell growth in a concentration-dependent manner (Fig. 4B).

The modification of RtH with [Chol][AA], however, seemed to have a significant effect on cell viability toward the two tested cell lines. A marked increase in cytotoxicity was recorded for all RtH–[Chol][AA]-complexes when they were tested against MCF-7 cells in comparison to that estimated for the native RtH. As can be seen in Fig. 3C, the cell viability was reduced by 60% and the activity of the protein complexes seemed to be independent on their concentration for all samples, except the RtH–[Chol][Gly]-complex. The antiproliferative activity of the cholinium glycinate–Hc complex depended strongly by the applied concentration. It is noteworthy to be mentioned that less than 5% of MCF-7 cells survived after 24 hour incubation with RtH–[Chol][Gly] at protein concentration of 700 $\mu g\ mL^{-1}$.

On the contrary, RtH–[Chol][Ile], RtH–[Chol][Leu] and RtH–[Chol][Met] applied in concentration up to 500 $\mu g\ mL^{-1}$ have a stimulatory effect on the embryonic fibroblast cells. The rest of samples slightly suppress the cell growth at these concentrations (Fig. 4C).

We assume that the enhanced antiproliferative activity of Hcs is due to a rearrangement in the protein secondary structure in which protein accommodates more appropriate conformation and interacts more specifically and closely with the cell surface. In addition, we assume that due to a partial protein denaturation a larger number of carbohydrate moieties become exposed to the protein surface. Similar dependence on (bio)polymer surface characteristics and conformations on their adsorption on fibrinogen as well as their effect on platelet adhesion/activation has been observed by Tzoneva *et al.*[34]

4. Conclusion

We found that all tested here cholinium amino acid salts induce significant re-arrangement of the secondary structure of the hemocyanin from *Rapana thomasiana*. The conformation and thermal stability of RtH depends strongly on the type of anion. Cellular activity of RtH–[Chol][AA] complexes is cell specific. The modified protein produces strong antiproliferative activity toward MCF-7 cells. The modified RtH has no significant effect or even in some cases enhances cell growth of normal fibroblast cells. Further investigations on the effect of other series of biocompatible ionic liquids on the structure and biological activity of Hcs are needed in order to reveal the mechanism of induced or enhanced anticancer activity.

References

1 J. Markl, *Biochim. Biophys. Acta, Proteins Proteomics*, 2013, **1834**, 1840–1852.
2 J. R. Harris and J. Markl, *Micron*, 1999, **30**, 597–623.
3 S. Arancibia, C. Espinoza, F. Salazar, M. D. Campo, R. Tampe, T.-Y. Zhong, P. de Ioannes, B. Moltedo, J. Ferreira, E. C. Lavelle, A. Manubens, A. E. de Ioannes and M. Becker, *PLoS One*, 2014, **9**, e87240.
4 V. Gesheva, S. Chausheva, N. Mihaylova, I. Manoylov, L. Doumanova, K. Idakieva and A. Tchorbanov, *BMC Immunol.*, 2014, **15**, 34–45.
5 D. Nillius, E. Jaenicke and H. Decker, *FEBS Lett.*, 2008, **582**, 749–754.
6 K. Idakieva, N. I. Siddiqui, F. Meersman, M. de Maeyer, I. Chakarska and C. Gielens, *Int. J. Biol. Macromol.*, 2009, **45**, 181–187.
7 H. Olivier-Bourbigou, L. Magna and D. Morvan, *Appl. Catal., A*, 2010, **373**, 1–56.
8 J. L. Shamshina, P. S. Barber and R. D. Rogers, *Expert Opin. Drug Delivery*, 2013, **10**, 1367–1381.
9 D. MacFarlane, N. Tachikawa, M. Forsyth, J. Pringle, P. C. Howlett, G. D. Elliott, J. H. Davis, Jr, M. Watanabe, P. Simon and C. Angell, *Energy Environ. Sci.*, 2014, 232–250.
10 M. Sureshkumar and C.-K. Lee, *J. Mol. Catal. B: Enzym.*, 2009, **60**, 1–12.
11 Z. Yang and W. Pan, *Enzyme Microb. Technol.*, 2005, **37**, 19–28.
12 N. Byrne and C. Austen Angell, *Chem. Commun.*, 2009, 1046–1048.
13 E. Yamamoto, S. Yamaguchi and T. Negamune, *Appl. Biochem. Biotechnol.*, 2011, **164**, 957–967.
14 M. Böhm, A. A. Tietze, P. l Heimer, M. Chen and D. Imhof, *J. Mol. Liq.*, 2014, **192**, 67–70.
15 K. Fujita, D. R. MacFarlane, M. Forsyth, M. Yoshizawa-Fujita, K. Murata, N. Nakamura and H. Ohno, *Biomacromolecules*, 2007, **8**, 2080–2086.
16 D. Constatinescu, C. Herrmann and H. Weingärtner, *Phys. Chem. Chem. Phys.*, 2010, **12**, 1756–1763.
17 A. Kumar and P. Venkatesu, *RSC Adv.*, 2013, **3**, 362–367.
18 A. Kumar and P. Venkatesu, *RSC Adv.*, 2014, **4**, 4487–4499.
19 A. Tietze, F. Bordusa, R. Giernoth, D. Imhof, T. Lenzer, A. Maaß, C. Mrestani-Klaus, I. Neundorf, K. Oum, D. Reith and A. Stark, *ChemPhysChem*, 2013, **14**, 4044–4064.
20 H. Weingärtner, C. Cabrele and C. Herrmann, *Phys. Chem. Chem. Phys.*, 2012, **14**, 415–426.
21 K. Idakieva, S. Severov, I. Svendsen, N. Genov, S. Stoeva, M. Beltramini, G. Tognon, P. Di Muro and B. Salvato, *Comp. Biochem. Physiol., Part B: Biochem. Mol. Biol.*, 1993, **106**, 53–59.
22 U. K. Laemmli, *Nature*, 1970, **227**, 680–685.
23 A. Natalello, D. Ami, S. Brocca, M. Lotti and S. M. Doglia, *Biochem. J.*, 2005, **385**, 511–517.
24 F. Secundo and G. Carrea, *Biotechnol. Bioeng.*, 2005, **92**, 438–446.
25 A. Barth, *Biochim. Biophys. Acta, Bioenerg.*, 2007, **1767**, 1073–1101.
26 T. Mosmann, *J. Immunol. Methods*, 1983, **65**, 55–63.
27 K. Idakieva, I. Chakarska, P. Ivanova, A. Tchorbanov, I. Dobrovolov and L. Doumanova, *Biotechnol. Biotechnol. Equip.*, 2009, **23**, 1364–1367.
28 A. Sanchez-Ferrer, J. N. Rodriguez-Lopez, F. Garcla-Canovas and F. Garcia-Carmona, *Biochim. Biophys. Acta, Protein Struct. Mol. Enzymol.*, 1995, **1247**, 1–11.

29 P. Attri, P. Venkatesu, A. Kumar and N. Byrne, *Phys. Chem. Chem. Phys.*, 2011, **13**, 17023–17026.
30 K. Idakieva, S. Stoeva, K. Pervanova, N. Genov and W. Voelter, *Biochim. Biophys. Acta, Protein Struct. Mol. Enzymol.*, 2000, **1479**, 175–184.
31 Y. Hu and X. Peng, Structure and Interactions of Ionic liquids, in *Effect of the structures of ionic liquids on their physical chemical properties*, ed. S. Zhang, J. Wang, Q. Zhao and Q. Zhou, Springer-Verlag Berlin Heidelberg, 2014, pp. 141–174.
32 D. Riggs, B. Jackson, L. Vona-Davis, A. Nigam and D. McFadden, *Am. J. Surg.*, 2005, **189**, 680–684.
33 W. Gouveia, T. F. Jorge, S. Martins, M. Meireles, M. Carolino, C. Cruz, T. V. Almeida and M. E. M. Araújo, *Chemosphere*, 2014, **104**, 51–56.
34 R. Tzoneva, M. Heuchel, T. Groth, G. Altankov, W. Albrecht and D. Paul, *J. Biomater. Sci., Polym. Ed.*, 2002, **13**, 1033–1050.